CONF-8908134--31

Proceedings of the 11th Int'l Conf. FELs, Naples, FL., August 1989

High Average Power CW FELs for Application to Plasma Heating: Designs and Experiments

J.H. Booske, V.L. Granatstein, D.J. Radack, T.M. Antonsen, Jr., S. Bidwell, Y. Carmel, W.W. Destler, P.E. Latham, B.Levush, I.D. Mayergoyz, and Z.X. Zhang

Laboratory for Plasma Research

University of Maryland, College Park, MD 20742

and

H.P. Freund

Science Applications International Corporation

McLean, VA 22102

CONF-8908134--31

DE90 011085

FG05-87ER 52147

Abstract

A short period wiggler (period ~ 1 cm), sheet beam FEL has been proposed as a low-cost source of high average power (1 MW) millimeter-wave radiation for plasma heating and space-based radar applications. Recent calculations and experiments have confirmed the feasibility of this concept in such critical areas as rf wall heating, intercepted beam ("body") current, and high voltage (0.5 - 1 MV) sheet beam generation and propagation. Results of preliminary low-gain sheet beam FEL oscillator experiments using a field emission diode and pulse line accelerator have verified that lasing occurs at the predicted FEL frequency. Measured start oscillation currents also appear consistent with theoretical estimates. Finally, we consider the possibilities of using a short-period, superconducting planar wiggler for improved beam confinement, as well as access to the high gain, strong pump Compton regime with its potential for highly efficient FEL operation.

INTRODUCTION

The use of a small period planar wiggler ($\ell_w \sim 1$ cm) Free Electron Laser (FEL) oscillator together with a sheet electron beam has been proposed as a low cost source of power for electron cyclotron resonance heating (ECRH) in magnetic fusion plasmas.[1] Other potential applications include space-based radar systems.[1] In previous work, we have established the feasibility of stable sheet beam confinement using wiggler focusing[2] and developed

The remaining agent for thermal stress of the cavity waveguide walls, then, is body current. Having already established that relativistic sheet beams propagate stably under wiggler-focusing,[1,2] we turned to the question of how much fractional body current would intercept the waveguide walls for a given set of design parameters. The various causes of beam interception include ballistic motion, space charge expansion, orbit perturbation by the rf radiation fields, and wiggler field errors. We will discuss the first three body current mechanisms in this paper. The effect of wiggler field errors will be addressed in a later publication.

A "Brillioun" equilibrium condition for wiggler confinement of a laminar sheet beam against space charge expansion can be derived as [2]

$$\omega_p^2 = \frac{\gamma^2}{2\gamma}\Omega_w^2 \tag{1}$$

where $\omega_p^2 = 4\pi ne^2/m$ and $\Omega_w = eB_w/mc$. For quantitative purposes, Eq. (1) can be written as

$$J_b(\mathrm{A/cm^2}) = 232\gamma\beta B_w^2 \tag{2}$$

where B_w, the wiggler field amplitude, is in kG and J_b is the "Brillioun" equilibrium current density. In all cases, our sheet beam FEL designs are specified such that the injected beam current density is less than one order of magnitude smaller than the Brillioun current density. Thus, the wiggler focusing forces greatly dominate the space charge forces and space charge is not a determining factor in fractional body currents.

Ballistic motion of single electron orbits can be conservatively estimated to follow the periodic betatron orbit solution[8]:

$$y(z) = \mathcal{Y}_\beta \sin\left(\frac{2\pi z}{\lambda_\beta} + \Psi_\beta\right) \tag{3}$$

where

$$\begin{aligned} \mathcal{Y}_\beta &= \sqrt{y_0^2 + \left(\frac{\lambda_\beta c_{y0}}{2\pi}\right)^2} \\ \Psi_\beta &= \tan^{-1}\left(\frac{2\pi y_0}{\lambda_\beta \theta_{y0}}\right) \\ \lambda_\beta &= \frac{m\gamma\beta c\sqrt{2}}{eB_w} \end{aligned}$$

and y_0 and θ_{y0} are the injected electron's transverse position and the divergence angle, respectively. Accordingly, electron interception of the waveguide wall will be avoided if the

of these experiments are described more fully in Ref. 11, we will summarize the results below. The modifications to the configuration of Ref. 2 included electrically isolating the waveguide body in order to measure small body currents, as well as replacing the series of small holes in the masking anode with a 1 mm thick rectangular slit. Thus, for these experiments the injected beam was a true sheet beam. By deliberate, careful experimental techniques, we obtained a minimum fractional body current resolution capability of $I_{body}/I_{beam} < 0.5\%$. The body currents were measured for 500 kV beams under two conditions: (1) a high current density ($J \sim 0.5$ - 1.5 kA/cm^2), large emittance ($\theta_{y0} \lesssim \pm 5°$) beam and (2) a low current density ($J \sim 7.5$ - 15 A/cm^2), low emittance ($\theta_{y0} \lesssim \pm 1°$) beam. The fractional body current data is plotted in Fig. 2. The "single anode beam" data corresponds to the high current density, large emittance conditions, while the "double anode beam" data corresponds to the low current density, low emittance conditions. The experimental results agreed well with the theoretical predictions in the following ways. First the "single anode beam" had a current density of order the Brillioun current density of Eq. (2). Furthermore, this same beam had a significant fraction of electron current which exceeded the ballistic confinement conditions of Eqs. (3) and (4). Consequently, as expected, roughly 20% body current was measured for this beam at wiggler fields as high as 2 kG. The "double anode beam", on the other hand, had a current density one order of magnitude less than the Brillioun value, as well as an injected electron emittance which satisfied the ballistic confinement condition of Eqs. (3) and (4) by a wide margin. Therefore, in agreement with predictions, the body current for this beam was essentially zero within the resolution of the measurement.

HIGH VOLTAGE SHEET BEAM THERMIONIC GUN DESIGN

From the previous discussion, one can determine that the proposed FEL will require a CW thermionic "Pierce" gun with an injected beam thickness $b_{beam} \sim 1$ mm, beam voltage $V_{beam} \sim 0.5$ - 1.0 MV, linear current density $i_{beam} \sim 7.5$ - 15.0 A/cm (area current density $J_{beam} \sim 75$ - 150 A/cm^2), and a maximum pitch angle at injection of $\theta_{beam} \lesssim \pm 2$ degrees. Present state-of-the-art[12] sets the maximum electric field for CW operation at $\sim$ 100 kV/cm. To realize the maximum FEL intrinsic (electronic) efficiency requires the beam energy spread in the interaction region to be $\Delta\gamma_z/(\gamma_z - 1) \leq \pm 2\%$.[3]

SHORT-PULSE, SHEET BEAM, SPW-FEL OSCILLATOR EXPERIMENTS

By adding a copper "end-cap" to the waveguide used in the beam transport experiments of Refs. 2 and 11, we converted the configuration to a low-gain, short-pulse oscillator. The oscillator configuration schematic is shown in Fig. 5. The same wiggler/cavity arrangement has been used in preliminary experiments on both 30 ns and 100 ns pulse-line accelerator injectors using field emission diodes. Neither beam pulse duration is sufficient for oscillator saturation. Furthermore, neither pulse has a sufficiently flat voltage pulse for optimum interaction efficiency. Nevertheless, initial lasing experiments on these systems provides us with useful information on lasing frequencies and start oscillation currents which can be compared with theoretical predictions.

The first experiments were performed on the same 30 ns pulse line accelerator used in the beam transport experiments of Refs. 2 and 11. A definite correlation between detected radiation and wiggler field intensity was established as shown in Fig. 6. These particular experiments were performed with a beam energy of approximately 300 kV and a beam current of approximately 100-150 A. Using waveguide cutoff filter techniques, it was established that the majority of the detected signal was in the 40-70 GHz frequency band. This is consistent with a grazing FEL interaction in a TE_{01} transverse waveguide mode for the particular experimental parameters. The same FEL oscillator configuration has been moved to a 100 ns pulse line accelerator system which has the capability of much flatter beam voltage during the pulse duration, provided a proper match is achieved between the diode and the injector's pulse transmission line. While this work is just getting underway, the preliminary data displayed in Fig. 7 indicates that start oscillation currents are of order 50 A. For the experimental parameters chosen, this would be in approximate agreement with the formula [3]

$$I_{start} \approx 15 \left(\frac{k_z \omega}{4\pi}\right) a_{rf} b_{rf} \left(\frac{mc^2}{e}\right) \left(\frac{c}{\omega}\right)^3 \frac{(\gamma_0^2 - 1)^{5/2} T_{eff}}{L^3 a_w^2 (1 + \frac{1}{2} a_w^2)}, \tag{6}$$

for an effective transmission coefficient of $T_{eff} \sim 0.01$. Measurements of the cavity transmission losses are presently in progress. Nevertheless, the small value of T_{eff} mentioned above would be consistent with the small output couping hole and masking anode slit used in the experiment.

Thus, both Eqs. (7) and (8) should be satisfied. For tapered efficiencies of 30-40%, the output power would be approximately 1.2-1.6 MW per device. If depressed collectors with spent beam collection efficiency of 60-70% were possible, the resulting total system efficiency would be approximately 50%. Finally, based on the linear gain estimates, using the sheet beam SPW FEL in an amplifier configuration would correspond to power amplification of 30 to 40 dB. Thus, an input gyrotron oscillator of 100-1000 W CW would be sufficient to achieve the desired 1 MW output power. We are presently studying the question of the actual length of such an amplifier design, including the tapering. Note that the sheet beam SPW amplifier should have the same low rf wall losses as predicted for the oscillator designs in Table 1. Furthermore, although the amplifier interaction region would be significantly longer than for the low-gain oscillator designs, the body current should still be manageable, due to the improved beam confinement and the lower total beam current associated with the SC wiggler FEL amplifier.

REFERENCES

1. V.L. Granatstein, T.M. Antonsen, Jr., J.H. Booske, W.W. Destler, P.E. Latham, B.Levush, I.D. Mayergoyz, D.J. Radack, Z.Segalov, and A. Serbeto, Nucl. Instr. Meth. Phys. Res. **A272**, 110 (1988).

2. J.H. Booske, W.W. Destler, Z. Segalov, D.J. Radack, E.T. Rosenbury, J. Rodgers, T.M. Antonsen, Jr., V.L. Granatstein, and I.D. Mayergoyz, J. Appl. Phys. **64**, 6 (1988).

3. J.H. Booske, A. Serbeto, T.M. Antonsen, Jr., and B. Levush, J. Appl. Phys. **65**, 1453 (1989).

4. J.H. Booske, V.L. Granatstein, T.M. Antonsen, Jr., W.W. Destler, J. Finn, P.E. Latham, B.Levush, I.D. Mayergoyz, D. Radack, J. Rodgers, M.E. Read, and A. Linz, Nucl. Instr. Meth. Phys. Res. (to be published, 1989).

5. T.M. Antonsen, Jr. and P.E. Latham, Phys. Fl. **31**, 3379 (1988).

6. T.M. Antonsen, Jr. and B. Levush, Phys. Fl. **B1**, 1097 (1989).

Table 1. 1 MW, 300 GHz Untapered FEL Oscillator Designs

V_{beam} (kV)	650	850	1000
I_{beam} (A)	48	40	34
b_{beam} (cm)[1]	0.20	0.24	0.26
a_{beam} (cm)	4.0	4.0	4.0
θ_{beam} (deg)	± 2.0	± 2.0	± 2.0
b_{rf} (cm)	0.375	0.575	0.70
a_{rf} (cm)	5.5	6.0	6.0
T_{eff}	0.13	0.11	0.12
L (cm)	19.6	25	30
ℓ_w (cm)	0.85	1.25	1.50
N_w (# periods)	23	20	20
B_w (kG)	2.0	2.0	2.0
λ_β (cm)	15.5	18.7	21.1
f (GHz)	285	288	300
η_e	3.0%	3.1%	3.0%
$\delta\gamma_z/(\gamma_z - 1)$ (total)	± 0.8%	± 0.8%	± 1.0%
beam/wall clearance (mm)	0.88	1.7	2.2
$\theta_{intercept}$ (deg)	± 3.5	± 5.5	± 6.0
$\hat{P}^{rf}_{wall}$ (W/cm^2)[2],[3]	72	24	< 10
P_{cav} (MW)	6.9	9.3	< 8.9
P_{out} (MW)	0.90	1.00	1.02
η_T (92% beam energy recovery)	28%	28%	28%
ϕ_{LV} (kV)	71.5	93.5	110

Notes:

(1) Injected beam thickness is 1 mm in all cases.

(2) Used σ-values reduced ×2 from textbook values.

(3) Maximum estimated cooling capability ~ 1.5 kW/cm^2.

FIGURE CAPTIONS

Fig. 1. Fractional body current contours in both energy-position phase space and pitch (divergence) angle versus position trace space. Data resulted from 3-D trajectory simulations for the 1 MV FEL design in Table 1. Point marked with a cross (+) is a conservation characterization of a predicted sheet beam gun design.

Fig. 2. Fractional body current for two ~ 500 kV sheet beams as a function of wiggler-focusing field amplitude. The "double anode beam" had much lower emittance and current density than the "single anode beam".

Fig. 3. Sample simulation of a 0.7-1.0 MV sheet beam thermionic gun design using multi-anode electrostatic focusing. The solution shown was a nonthermal solution based on 14 rays. Little change was found when using more rays (up to 98) or by varying the final anode voltage over a ~ 200-300 kV range.

Fig. 4. Trace space for both non-thermal (open squares) and (3 eV) thermal (dark circles) beam solutions of the gun in Fig. 3. The solid boundary represents the analytic ballistic confinement limit for the 850 kV FEL design using a 2 kG (i.e., room temperature) wiggler. The dashed boundary is the same confinement limit using a 6 kG (superconducting) wiggler.

Fig. 5. SPW sheet beam FEL oscillator configuration used in preliminary experiments with a pulse-line accelerator injector.

Fig. 6. Correlation between FEL radiation detector signal and wiggler field strength. (a) B_w = 0 kG, (b) B_w = 0.8 kG, (c) B_w = 1.5 kG.

Fig. 7. Correlation between FEL radiation detector signal and collected beam current, indicating a start oscillation current of approximately 50 A.

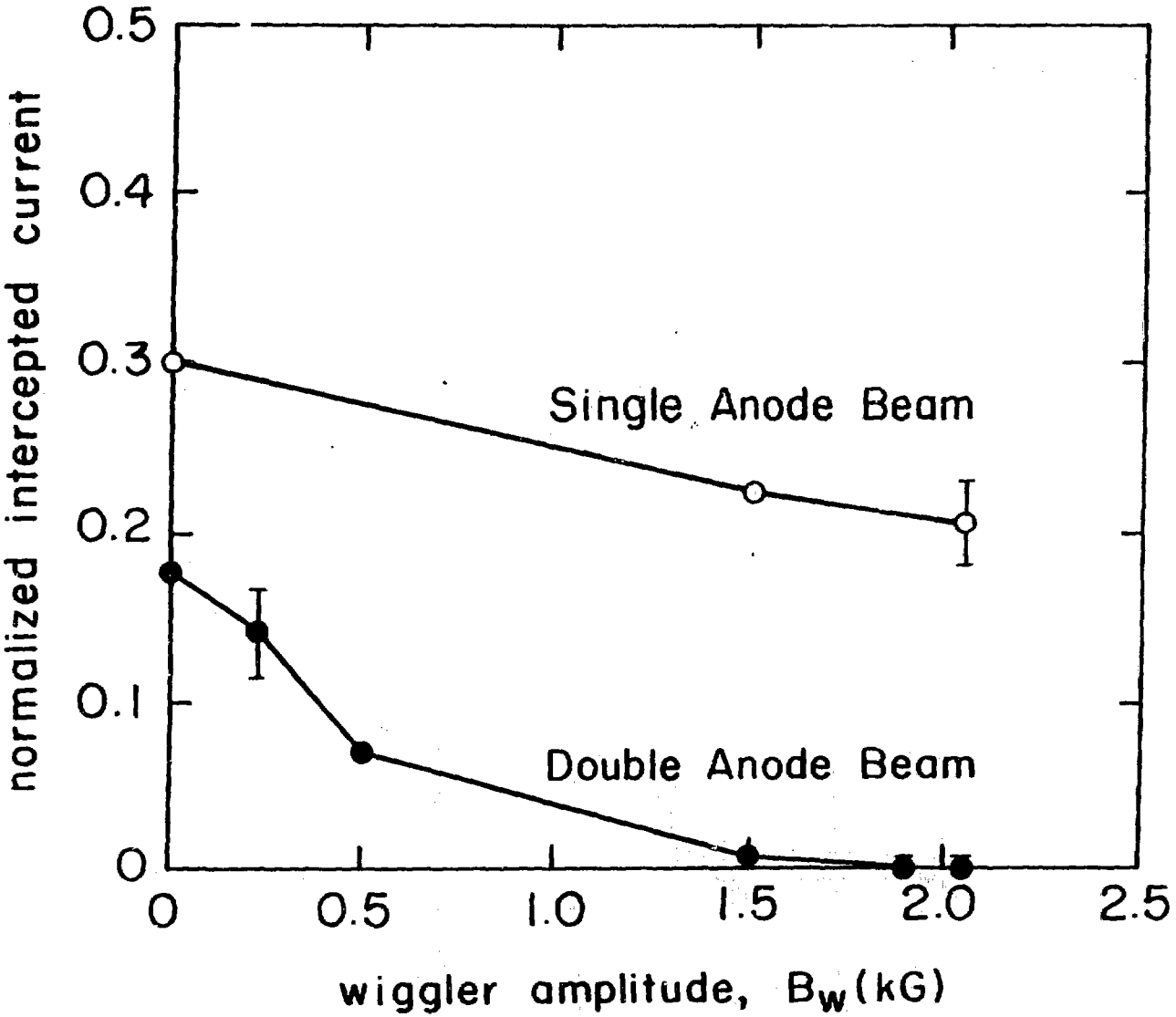
0.5
0.4
0.3
0.2
0.1
0
normalized intercepted current
Single Anode Beam
Double Anode Beam
0
0.5
1.0
1.5
2.0
2.5
wiggler amplitude, B_w(kG)

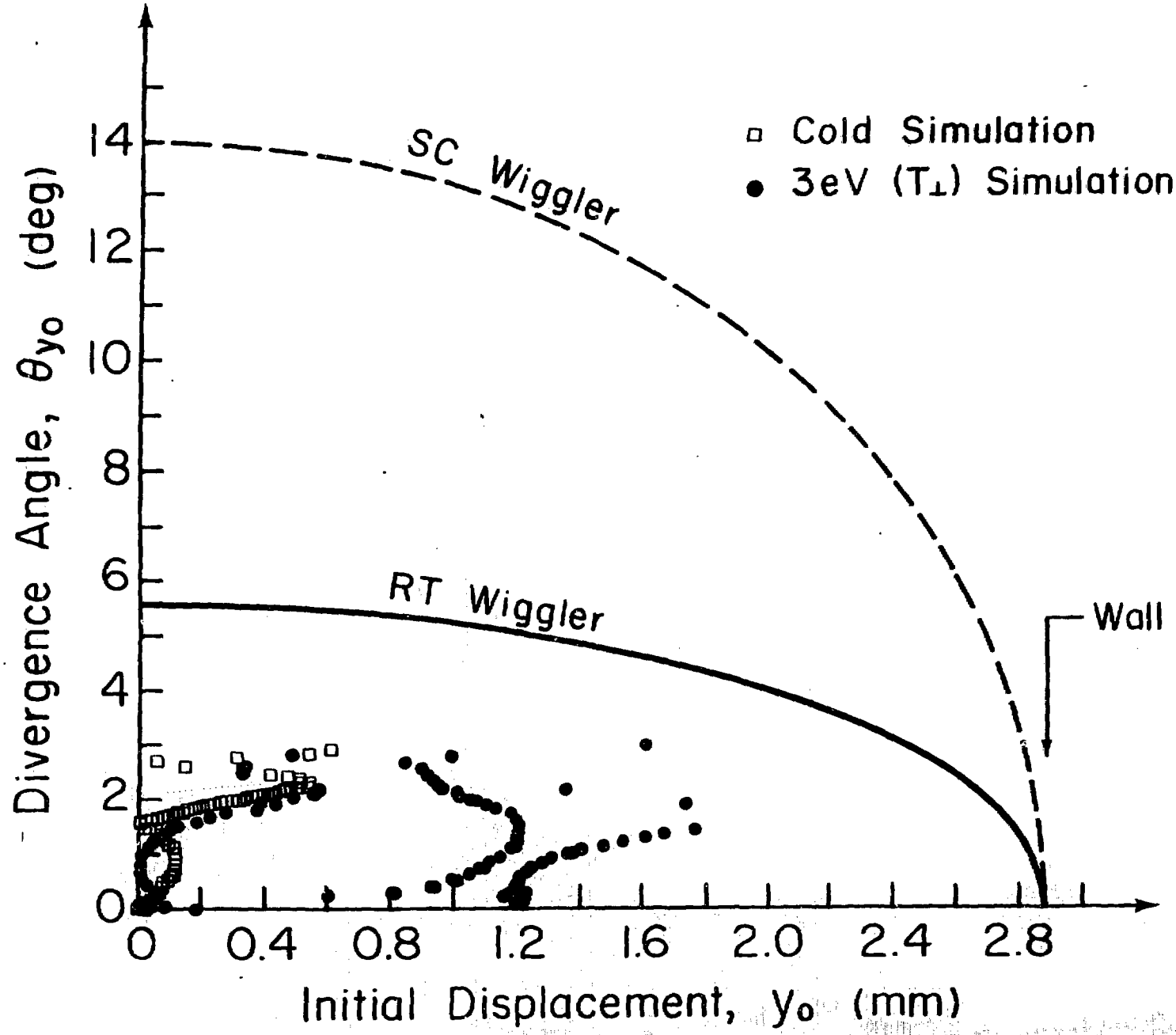
Cold Simulation
3eV ($T_\perp$) Simulation
SC Wiggler
RT Wiggler
Wall
Divergence Angle, θ_{yo} (deg)
0
2
4
6
8
10
12
14
0
0.4
0.8
1.2
1.6
2.0
2.4
2.8
Initial Displacement, y_o (mm)

Fig. 6